RAPID COMMUNICATIONS

PHYSICAL REVIEW B **79**, 100509(R) (2009)

Electrothermal feedback in superconducting nanowire single-photon detectors

Andrew J. Kerman,[1] Joel K. W. Yang,[2] Richard J. Molnar,[1] Eric A. Dauler,[1,2] and Karl K. Berggren[2]
[1]*Lincoln Laboratory, Massachusetts Institute of Technology, Lexington, Massachusetts 02420, USA*
[2]*Research Laboratory of Electronics, Massachusetts Institute of Technology, Cambridge, Massachusetts 02139, USA*
(Received 5 December 2008; revised manuscript received 30 January 2009; published 26 March 2009)

We investigate the role of electrothermal feedback in the operation of superconducting nanowire single-photon detectors (SNSPDs). It is found that the desired mode of operation for SNSPDs is only achieved if this feedback is unstable, which happens naturally through the slow electrical response associated with their relatively large kinetic inductance. If this response is sped up in an effort to increase the device count rate, the electrothermal feedback becomes stable and results in an effect known as latching, where the device is locked in a resistive state and can no longer detect photons. We present a set of experiments which elucidate this effect and a simple model which quantitatively explains the results.

DOI: 10.1103/PhysRevB.79.100509 PACS number(s): 85.25.Oj, 74.78.−w, 85.60.Gz

Superconducting nanowire single-photon detectors (SNSPDs) combine high speed, high detection efficiency (DE) over a wide range of wavelengths, and low dark counts.[1–4] Of particular importance is their high *single-photon* timing resolution of ~30 ps,[4] which permits extremely high data rates in photon-counting communications applications.[5,6] Full use of this electrical bandwidth is limited, however, by the fact that the maximum count rates of these devices are much smaller (a few hundred MHz for 10 μm^2 active area and decreasing as the area is increased[2]), limited by their large kinetic inductance and the input impedance of the readout circuit.[2,7] To increase the count rate, therefore, one must either reduce the kinetic inductance (by using a smaller active area or different materials or substrates) or increase the load impedance.[7] However, either of these approaches causes the wire to "latch" into a stable resistive state where it no longer detects photons.[8] This effect arises when negative electrothermal feedback, which in normal operation allows the device to reset itself, is made fast enough that it becomes stable. We present experiments which probe the stability of this feedback, and we develop a model which quantitatively explains our observations.

The operation of an SNSPD is illustrated in Fig. 1(a). A nanowire (typically ~100 nm wide and 5nm thick) is biased with a dc current I_0 near its critical current I_c. The nanowire has kinetic inductance L and is read out using a load impedance R_L (typically a 50Ω transmission line). When a photon is absorbed, a short (<100 nm long) normal domain is nucleated, giving the wire a resistance $R_n(t)$. This results in Joule heating which causes the normal domain (and consequently, R_n) to expand in time exponentially. The expansion is counteracted by negative electrothermal feedback from the load R_L, which forms a current divider with R_n, and diverts a current I_L into the load (so that the current in the nanowire is reduced to $I_d \equiv I_0 - I_L$), reducing the heating. However, in a correctly functioning device, this feedback is unstable: the inductive time constant is long enough so that before I_L becomes appreciable, Joule heating has already increased R_n, so that $R_n \gg R_L$. The current I_d then drops nearly to zero, turning off the heating and allowing the nanowire to quickly cool down and return to the superconducting state, after which I_d recovers with a time constant $\tau_e \equiv L/R_L$.[2] If one attempts to shorten τ_e too much, the negative feedback becomes fast enough to counterbalance the Joule heating before it runs away, resulting in a stable resistive domain, known as a self-heating hotspot.[9,10]

In a standard treatment of these hotspots,[9] solutions to a one-dimensional heat equation are found in which a normal-superconducting (NS) boundary propagates at constant velocity $v_{\rm NS}$ for fixed device current I_d.[9,11] This results in a solution of the form

$$v_{\rm NS} = v_0 \frac{\alpha (I_d/I_c)^2 - 2}{\sqrt{\alpha (I_d/I_c)^2 - 1}} \approx \frac{1}{\gamma}(I_d^2 - I_{\rm ss}^2), \qquad (1)$$

where $v_0 \equiv \sqrt{A_{\rm cs}\kappa h}/c$ is a characteristic velocity ($A_{\rm cs}$ is the wire's cross-sectional area, κ is its thermal conductivity, and c and h are the heat capacity and heat transfer coefficient to the substrate, per unit length, respectively), I_c is the critical current, and $\alpha \equiv \rho_n I_c^2 / h(T_c - T_0)$ is known as the Stekly parameter, which characterizes the ratio of Joule heating to

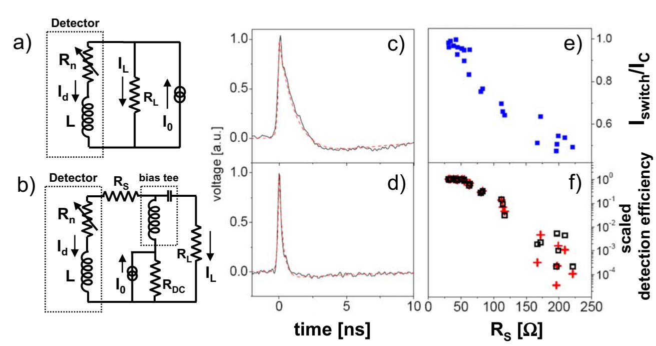

FIG. 1. (Color online) Speedup and latching of nanowire detectors with increased load impedance. (a) electrical model of detector operation. A hotspot is nucleated by absorption of a photon, producing a resistance R_n in series with the wire's kinetic inductance L. (b) Experimental circuit, including series resistor R_S, bias tee, and impedance of current source $R_{\rm dc}$. (c) and (d) Averaged pulse shapes for $R_S = 0, 250\Omega$ ($L \sim 50$ nH); dashed lines are predictions with no free parameters. (e) $I_{\rm switch}$ vs R_S. As R_S is increased, $I_{\rm switch}$ decreases, becoming less than I_c. (f) DE at $I_0 = 0.975 I_{\rm switch}$ vs R_S (open squares). Also shown (crosses) are the expected DEs assuming that latching affects DE simply by limiting I_0 (obtained from DE vs I_0 at $R_S = 0$).

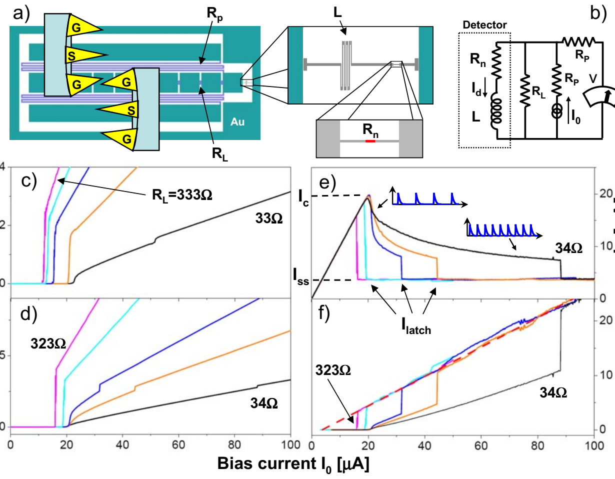

FIG. 2. (Color online) Hotspot stability measurements. (a) Device schematic; two ground-signal-ground probes perform a high-impedance three-point measurement of R_n, with R_L determined by probe position. (b) Equivalent electrical circuit. (c) and (d) Example *V-I* curves, with $L=60$ nH and $L=605$ nH, respectively. (e) and (f) Inferred I_d and R_n/R_L for the data shown in (d). In (e) the relaxation oscillations in the region $I_c<I_0<I_{\mathrm{latch}}$ are shown schematically. Dashed lines show (e) $I_d=I_c$ and $I_d=I_{\mathrm{ss}}$. (f) $R_{\mathrm{ss}}=R_L(I_0/I_{\mathrm{ss}}-1)$.

conduction cooling in the normal state[9] (ρ_n is the normal resistance of the wire per unit length and T_0 and T_c are the substrate and critical temperatures). Equation (1) is valid when $T_0 \ll T_c$, and the approximate equality holds when $|I_d-I_{\mathrm{ss}}| \ll I_{\mathrm{ss}}$ with $\gamma \equiv (T_c-T_0)(c/\rho_n)\sqrt{h/\kappa A_{\mathrm{cs}}}$ and $I_{\mathrm{ss}}^2 \equiv 2h(T_c-T_0)/\rho_n$. The physical meaning of Eq. (1) is clear: the NS boundary is stationary only if the local power density ($\propto I_d^2$) is equal to a fixed value; if it is greater, the hotspot will expand ($v_{\mathrm{NS}}>0$), if less it will contract ($v_{\mathrm{NS}}<0$).

We can use Eq. (1) to describe the electrothermal circuit in Fig. 1(a), by combining it with the circuit equation $I_dR_n+LdI_d/dt=R_L(I_0-I_d)$ (where $dR_n/dt=2\rho_n v_{\mathrm{NS}}$). To determine when the device will latch, we analyze the stability of the resulting second-order nonlinear system for small deviations from its steady-state solution $[I_d \rightarrow I_{\mathrm{ss}}, R_n \rightarrow R_L(I_0/I_{\mathrm{ss}}-1) \equiv R_{\mathrm{ss}}]$ to obtain a damping coefficient $\zeta = \frac{I_0}{4I_{\mathrm{ss}}}\sqrt{\tau_{\mathrm{th}}/\tau_e}$, where $\tau_{\mathrm{th}} \equiv R_L/2\rho_n v_0$ is a thermal time constant. This can be re-expressed in terms of $R_{\mathrm{tot}} \equiv R_L+R_{\mathrm{ss}}$ thus: $\zeta = \frac{1}{4}\sqrt{\tau_{\mathrm{th,tot}}/\tau_{e,\mathrm{tot}}}$ ($\tau_{e,\mathrm{tot}} \equiv L/R_{\mathrm{tot}}$ and $\tau_{\mathrm{th,tot}} \equiv R_{\mathrm{tot}}/2\rho_n v_0$), which clearly shows that the stability is determined by a ratio of electrical and thermal time constants.

In normal device operation, where the damping ζ is small, the feedback cannot stabilize the hotspot during the initial photoresponse, as described above. However, as I_0 is increased, ζ increases, making the hotspot more stable (this occurs because $R_{\mathrm{ss}} \propto I_0$ and larger R_{ss} gives a shorter inductive time constant $\tau_{e,\mathrm{tot}}$). Eventually, at a bias current $I_0=I_{\mathrm{latch}}$ the device latches. For a correctly functioning device, $I_{\mathrm{latch}}>I_c$, so that latching does not affect its operation. However, if τ_e is decreased, I_{latch} decreases, and eventually it becomes less than I_c. This prevents the device from being biased near I_c, resulting in a drastic reduction in performance.[12]

Devices used in this work were fabricated from ~5-nm-thick NbN films, deposited on *R*-plane sapphire substrates in a UHV dc magnetron sputtering system (base pressure $<10^{-10}$ mbar). Film deposition was performed at a wafer temperature of ~800 °C and a pressure of $\sim 10^{-8}$ mbar.[13] Aligned photolithography and liftoff were used to pattern ~100-nm-thick Ti films for on-chip resistors[8] and Ti:Au contact pads. Patterning of the NbN was then performed with *e*-beam lithography.[3] Devices were tested in a cryogenic probing station at 2 K as described in Refs. 2 and 3.

Figures 1(c)–1(f) show data for a set of (3 μm $\times 3.3$ μm area) devices having various resistors R_S in series with the 50Ω readout line[8] [Fig. 1(b)], so that $R_L=50\Omega+R_S$. For $R_S=0$, these devices had similar performance to those in Ref. 3. Panels (c) and (d) show averaged pulse shapes for devices with $R_S=0,250\Omega$, respectively. Clearly, the reset time can be reduced; however, this comes at a price. Panels (e) and (f) show, for devices with different R_S, the current $I_{\mathrm{switch}} \equiv \min(I_c, I_{\mathrm{latch}})$ above which each device no longer detects photons and the measured DE at $I_0=0.975I_{\mathrm{switch}}$. The data show that as R_S is increased, I_{switch} decreases far below I_C (due to reduction in I_{latch}), resulting in a significantly reduced DE.[14]

To investigate the latched state, we fabricated devices designed to probe the stability of self-heating hotspots as a function of I_0, L, and R_L. Each device consisted of three sections in series, as shown in Fig. 2(a): a 3-μm-long 100-nm-wide nanowire where the hotspot was nucleated, a wider (200 nm) meandered section acting as an inductance, and a series of nine contact pads interspersed with Ti-film resistors. Also shown are the two electrical probes, which result in the circuit of Fig. 2(b): a high-impedance ($R_p=20$ kΩ) three-point measurement of R_{ss}. We varied R_L by moving the probes along the line of contact pads and L by testing different devices (with different L). We tested 66 devices on three chips and selected from these only unconstricted[12] nanowires with nearly identical linewidths ($I_c \approx 22-24$ μA) and with $R_L=20\Omega-1000\Omega$ and $L=6-600$ nH.

For each L and R_L, we acquired a dc *V-I* curve like those shown in Figs. 2(c) and 2(d), sweeping I_0 downward starting from high values where the hotspot was stable.[15] These data can be converted to I_d and R_n, as shown in Figs. 2(e) and 2(f) [for the data of Fig. 2(d)]. From data of this kind, I_{latch} can be identified by the sudden jumps in I_d: for $I_0>I_{\mathrm{latch}}$, I_d is fixed (at I_{ss}), independent of I_0 and R_L, as predicted by Eq. (1).[16] For the largest values of R_L, I_d never reaches I_c [shown by a horizontal dashed line in Fig. 2(e)] because once it latches $I_d \rightarrow I_{\mathrm{ss}}<I_c$. As R_L is decreased, I_{latch} increases as expected, until another feature appears when $I_{\mathrm{latch}}>I_c$. In this region ($I_c<I_0<I_{\mathrm{latch}}$) the nanowire can neither superconduct nor latch and instead undergoes relaxation oscillations,[9,17] as indicated in the figure, producing a periodic pulse train with a frequency that increases as I_0 is increased.[14] The average resistance (from the dc *V-I* curve) increases with this frequency, producing the observed continuous decrease in I_d until I_{latch} is reached.

The data in Fig. 3 show the measured I_{latch} as R_L and L are varied, plotted in dimensionless form as $2\tau_e/\tau_{\mathrm{th}}(\propto L/R_L^2)$ vs $(I_{\mathrm{latch}}/I_{\mathrm{ss}})^2$, which can be thought of as defining the boundary between stable and unstable hotspots. Our simple model de-

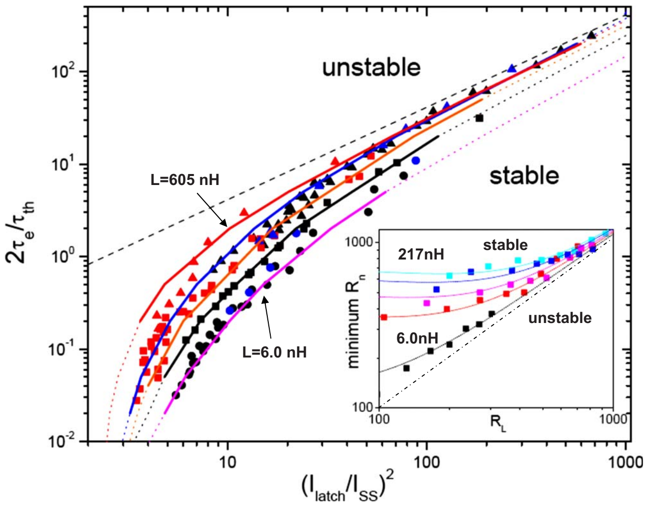

FIG. 3. (Color online) Summary of hotspot stability results. Data are shown from three different chips (indicated by different colors). Circles, squares, and triangles are data for $L=6-12$, 15–60, and 120–600 nH, respectively. In the $\tau_e \gg \tau_a$ limit (where NS domain-wall motion dominates the feedback), the data approach the dashed line, which is the prediction based on Eq. (1). The solid curves are obtained from Eq. (8) with a phase margin of 30°; each curve corresponds to a fixed L in the set (6,15,30,60,600) nH and spans the range of R_L in the data. The dotted lines extend these predictions over a wider range of R_L. For $\tau_e \ll \tau_{\mathrm{th}}$ the NS domain walls are effectively fixed and the temperature feedback dominates. In this regime the feedback is always unstable when $R_n \lesssim R_L$ (or equivalently, $I_0 \lesssim 2I_{\mathrm{ss}}$), as shown in the inset; the minimum stable R_n are all above the dashed-dotted line ($R_n = R_L$).

scribed above predicts a line of slope 1 (indicated by the dashed line). The data do approach this line, although only in the $\tau_e \gg \tau_{\mathrm{th}}$ limit. This is consistent with the assumption of constant (or slowly varying) I_d under which Eq. (1) was derived. As $\tau_e/\tau_{\mathrm{th}}$ is decreased, the data trend downward, away from this line, and $I_{\mathrm{latch}}/I_{\mathrm{ss}}$ becomes *almost independent of* $\tau_e/\tau_{\mathrm{th}}$ (all data approach the same vertical asymptote); this implies a minimum $I_{\mathrm{latch}}/I_{\mathrm{ss}}$, or equivalently, a minimum R_n/R_L, below which the hotspot is *always* unstable. This is shown in the inset: the measured minimum stable R_n is always greater than $\sim R_L$, over a range of L values from 6 to 217 nH (shown by solid symbols—solid lines are guides for the eyes).

This behavior can be explained in terms of a time scale τ_a over which the temperature profile of the hotspot stabilizes into the quasisteady-state form which yields Eq. (1). For power-density variations faster than this, the NS boundaries do not have time to start moving, resulting instead in a temperature deviation ΔT. Since the NS boundary occurs at $T \approx T_c$, where ρ_n is strongly temperature dependent (defined by $d\rho/dT \equiv \beta > 0$), this changes R_n, giving a second parallel electrothermal feedback path which dominates for frequencies $\omega \gg \tau_a^{-1}$. We can describe this by replacing Eq. (1) with

$$\frac{\gamma\rho_n}{2}\left(\tau_a \frac{d^2 l}{dt^2} + \frac{dl}{dt}\right) = I_d^2 \rho(\Delta T) - I_{\mathrm{ss}}^2 \rho_n, \tag{2}$$

$$c\frac{d\Delta T}{dt} = \frac{\gamma\rho_n\tau_a}{2}\frac{d^2 l}{dt^2} - h\Delta T. \tag{3}$$

Here, l is the hotspot length, $\rho(\Delta T)$ is the resistance per unit length [with $\rho(0) \equiv \rho_n$], and $R_n = \rho(\Delta T) l$. In Eq. (2), τ_a is the characteristic time over which $2v_{\mathrm{NS}} = dl/dt$ adapts to changes in power density: for slow time scales $dt \gg \tau_a$, we have $\tau_a d^2 l/dt^2 \ll dl/dt$ and Eq. (2) reduces to Eq. (1) (with $\Delta T = 0$). For faster time scales, $\tau_a d^2 l/dt^2$ becomes appreciable and acts as a source term for temperature deviations in Eq. (3). When $dt \ll \tau_a$, $\tau_a d^2 l/dt^2 \gg dl/dt$ and Eqs. (2) and (3) can be combined to give $c \cdot d\Delta T/dt \approx I_d^2 \rho(\Delta T) - I_{\mathrm{ss}}^2 \rho_n - h\Delta T$.[18] In this limit, if $R_L \lesssim R_n$ the bias circuit including R_L begins to look like a current source, which then results in positive feedback: a current change produces a temperature and resistance change of the same sign. Therefore, the hotspot is always unstable when $R_n \lesssim R_L$.

Expressing Eqs. (2) and (3) in dimensionless units ($i \equiv I_d/I_0$, $r \equiv R_n/R_L$, $\lambda \equiv l\beta T_c/R_L$, and $\theta \equiv T/T_c$) and expanding to first order in small deviations ($\delta i, \delta r, \delta\lambda, \delta\theta$) from steady state, we obtain

$$\delta i' = -(i_0 \delta i + i_0^{-1} \delta r), \tag{4}$$

$$\delta r = \eta(i_0 - 1)\delta\theta + \eta^{-1}\delta\lambda, \tag{5}$$

$$\frac{\tau_a}{\tau_e}\delta\lambda'' + \delta\lambda' = 2\eta^2 \frac{\tau_e}{\tau_{\mathrm{th}}}(\delta\theta + 2 i_0 \eta^{-1} \delta i), \tag{6}$$

$$\delta\theta' = \frac{\Theta \tau_{\mathrm{th}} \tau_a}{\eta \tau_e \tau_c}\delta\lambda'' - \frac{\tau_e}{\tau_c}\delta\theta. \tag{7}$$

Here, the prime denotes differentiation with respect to t/τ_e, $i_0 \equiv I_0/I_{\mathrm{ss}}$, $\Theta \equiv (T_c - T_0)/T_c$, $\eta \equiv \beta T_c/\rho_n$ characterizes the resistive transition slope, and $\tau_c \equiv c/h$ is a cooling time constant. When $\tau_e \gg \tau_{\mathrm{th}}, \tau_a$, the system reduces to $\delta i'' + i_0 \delta i' - 4\tau_e/\tau_{\mathrm{th}} \approx 0$, which has damping coefficient $\zeta = i_0 (4\sqrt{\tau_e/\tau_{\mathrm{th}}})^{-1}$, as above. In the opposite limit, where $\tau_e \ll \tau_{\mathrm{th}}, \tau_a$, we obtain $\delta i'' + i_0 \delta i' + (2\eta\Theta\tau_e/\tau_c)(i_0 - 2) \approx 0$. In agreement with our argument above, the oscillation frequency becomes negative for $R_n < R_L$ ($I_0 < 2I_{\mathrm{ss}}$).

We characterize the stability of the system of Eqs. (4)–(7) using its "open loop" gain A_{ol}: we assume a small oscillatory perturbation by replacing δr in Eq. (4) with $\Delta r e^{j\omega t}$ and responses $(\delta i, \delta\theta, \delta\lambda, \delta r)e^{j\omega t}$. Solving for $A_{\mathrm{ol}} \equiv \delta r/\Delta r$, we obtain

$$A_{\mathrm{ol}} = \frac{4\frac{\tau_e}{\tau_{\mathrm{th}}}\left(1 + j\omega\frac{\tau_c}{\tau_e}\right) - 4\eta\Theta\omega^2(i_0 - 1)\frac{\tau_a}{\tau_e}}{j\omega i_0\left(1 + \frac{j\omega}{i_0}\right)\left[2j\omega\eta\Theta\frac{\tau_a}{\tau_e} - \left(1 + j\omega\frac{\tau_c}{\tau_e}\right)\left(1 + j\omega\frac{\tau_a}{\tau_e}\right)\right]}. \tag{8}$$

The stability of the system can then be quantified by the phase margin $\pi + \arg[A_{\mathrm{ol}}(\omega_0)]$, where ω_0 is the unity gain ($|A_{\mathrm{ol}}| = 1$) frequency. In the extreme case, when the phase margin is zero ($\arg[A_{\mathrm{ol}}(\omega_0)] = -\pi$), the feedback is positive. The solid lines in Fig. 3 show our best fit to the data. Note that although the stability is determined only by $\tau_e/\tau_{\mathrm{th}}$ and i_0 in the two extreme limits (not visible in the figure), in the intermediate region of interest here this is not the case, so several curves are shown. Each solid curve segment corresponds to a single L, over the range of R_L tested; the dotted lines continue these curves for a wider range of R_L. The data are grouped into three inductance ranges: 6–12, 15–60, and 120–600 nH, indicated by circles, squares, and triangles, respectively. We used fixed values $\Theta=0.8$ and $\eta=6.5$, which are based on independent measurements, and fitted $\tau_a=1.9$ ns and $\tau_c=0.47$ ns to all data.[19] Separate values of $\rho_n v_0$ were fitted to data from each of the three chips, differing at most by a factor of ~ 2. These fitted values were $\rho_n v_0 \sim 1\times 10^{11}$ Ω/s; since $\rho_n \sim 3\times 10^{9}$ Ω/m, this gives $v_0 \sim 30$ m/s, which is a reasonable value.

A natural question to ask in light of this analysis is whether it suggests a method for speeding up these devices. The most obvious way would be to increase the heat transfer coefficient h, which increases both I_{ss} and v_0, moving the wire further into the unstable region and allowing its speed to be increased further without latching. However, at present it is unknown how much h can be increased before the DE begins to suffer. At some point, the photon-generated hotspot will disappear too quickly for the wire to respond in the desired fashion. In any case, experiments like those described here will be a useful measurement tool in future work for understanding the impact of changes in the material and/or substrate on the thermal coupling and electrothermal feedback.

We acknowledge helpful discussions with Sae Woo Nam, Aaron Miller, and Enectalí Figueroa-Feliciano. This work is sponsored by the United States Air Force under Contract No. FA8721-05-C-0002.

[1] G. Gol'tsman, O. Minaeva, A. Korneev, M. Tarkhov, I. Rubtsova, A. Divochiy, I. Milostnaya, G. Chulkova, N. Kaurova, B. Voronov, D. Pan, J. Kitaygorsky, A. Cross, A. Pearlman, I. Komissarov, W. Slysz, M. Wegrzecki, P. Grabiec, and R. Sobolewski, IEEE Trans. Appl. Supercond. **17**, 246 (2007); J. A. Stern and W. H. Farr, *ibid.* **17**, 306 (2007); F. Marsili, D. Bitauld, A. Gaggero, R. Leoni, F. Mattioli, S. Hold, M. Benkahoul, F. Levy, and A. Fiore, European Conference on Lasers and Electro-Optics 2007, p. 816; S. N. Dorenbos, E. M. Reiger, U. Perinetti, V. Zwiller, T. Zijlstra, and T. M. Klapwijk, Appl. Phys. Lett. **93**, 131101 (2008); A. D. Semenov, P. Haas, B. Günther, H.-W. Hübers, K. Il'in, M. Siegel, A. Kirste, J. Beyer, D. Drung, T. Schurig, and A. Smirnov, Supercond. Sci. Technol. **20**, 919 (2007); S. Miki, M. Fujiwara, M. Sasaki, B. Baek, A. J. Miller, R. H. Hadfield, S. W. Nam, and Z. Wang, Appl. Phys. Lett. **92**, 061116 (2008).

[2] A. J. Kerman, E. A. Dauler, W. E. Keicher, J. K. W. Yang, K. K. Berggren, G. N. Gol'tsman, and B. M. Voronov, Appl. Phys. Lett. **88**, 111116 (2006).

[3] K. M. Rosfjord, J. K. W. Yang, E. A. Dauler, A. J. Kerman, V. Anant, B. M. Voronov, G. N. Gol'tsman, and K. K. Berggren, Opt. Express **14**, 527 (2006).

[4] E. A. Dauler, A. J. Kerman, B. S. Robinson, J. K. W. Yang, B. Voronov, G. Gol'tsman, S. A. Hamilton, and K. K. Berggren, J. Mod. Opt. **56**, 364 (2009).

[5] D. Rosenberg, S. W. Nam, P. A. Hiskett, C. G. Peterson, R. J. Hughes, J. E. Nordholt, A. E. Lita, and A. J. Miller, Appl. Phys. Lett. **88**, 021108 (2006); H. Takesue, S. W. Nam, Q. Zhang, R. H. Hadfield, T. Honjo, K. Tamaki, and Y. Yamamoto, Nat. Photonics **1**, 343 (2007).

[6] B. S. Robinson, A. J. Kerman, E. A. Dauler, D. M. Boroson, S. A. Hamilton, J. K. W. Yang, V. Anant, and K. K. Berggren, Proc. SPIE **6709**, 67090Z (2007).

[7] A potential alternative has recently been demonstrated by A. Korneev, A. Divochiy, M. Tarkhov, O. Minaeva, V. Seleznev, N. Kaurova, B. Voronov, O. Okunev, G. Chulkova, I. Milostnaya, K. Smirnov, and G. Gol'tsman, J. Phys.: Conf. Ser. **97**, 012307 (2008), although latching may affect this as well.

[8] J. K. W. Yang, A. J. Kerman, E. A. Dauler, V. Anant, K. M. Rosfjord, and K. K. Berggren, IEEE Trans. Appl. Supercond. **17**, 581 (2007).

[9] A. Vl. Gurevich and R. G. Mints, Rev. Mod. Phys. **59**, 941 (1987), and references therein.

[10] Since the negative feedback opposes the fast joule heating that produces the rising edge of the output pulse, it may also affect the timing jitter of this edge.

[11] This description is further simplified by the fact that near the NS boundary all material properties can be approximated by their values at T_c.

[12] A. J. Kerman, E. A. Dauler, J. K. W. Yang, K. M. Rosfjord, V. Anant, K. K. Berggren, G. N. Gol'tsman, and B. M. Voronov, Appl. Phys. Lett. **90**, 101110 (2007).

[13] R. J. Molnar, E. A. Dauler, A. J. Kerman, and K. K. Berggren (unpublished).

[14] For the circuit in Fig. 1(b), if $I_{latch} > I_c$, the detector oscillates [see Fig. 2(e) and associated discussion] for the time constant of the bias tee, after which it senses the larger $R_{dc}=5$ kΩ and latches. The absence of this burst of pulses is a signature for $I_{latch} < I_c$.

[15] The results were almost identical when sweeping I_0 upward, since the dark counts of the device allow it to lock into the latched state if it is stable.

[16] From the observed $I_{ss}\approx 5$ μA and $\rho_n \sim 3\times 10^{9}$ Ω m^{-1}, Eq. (1) gives $h\sim 5\times 10^{-3}$ W m^{-1} K^{-1}; this gives $\alpha \sim 30$ ($T_C\approx 10$ K, $T_0=2$ K, and $I_C=22$ μA).

[17] R. H. Hadfield, A. J. Miller, S. W. Nam, R. L. Kautz, and R. E. Schwall, Appl. Phys. Lett. **87**, 203505 (2005).

[18] This equation is identical to that governing a transition-edge sensor under the action of negative electrothermal feedback; see, e.g., K. D. Irwin, G. C. Hilton, D. A. Wollman, and J. M. Martinis, J. Appl. Phys. **83**, 3978 (1998).

[19] From the fitted $\tau_c=0.47$ ns and the h inferred above (Ref. 16), we obtain $c=2.2\times 10^{-12}$ J m^{-1} K^{-1}. Reference 8 gives $c_{el}=1.2\times 10^{-12}$ and $c_{ph}=4.9\times 10^{-12}$ J m^{-1} K^{-1}.